Men's Artistic Gymnastics: Anew high bar - gymnast model with sensitivity analysis

S Linge, Telemark University College

Abstract

The purpose of this work[1] was to develop a new 2D gymnast - high bar model with horizontal bar endpoint dynamics included. To this end, a three-spring high bar model was extended with a 5 segment gymnast model followed by validation and sensitivity analysis. Validation over a complete giant swing was favourable (bar position rms errors $< 0.017\,m$, centre of mass angular position rms error $< 11°$). Single parameter perturbations (10%) caused little deterioration in model performance (lower half of giant swing, - bar position rms errors $< 0.006\,m$, arms' angle rms error $< 0.9°$). Combinations of parameter perturbations gave bar position rms errors $< 0.008\,m$ and arms' angle rms error $< 1.8°$. Model performance was most sensitive to errors in high bar stiffness values.

1 Introduction

Modeling and simulation has previously been used to study several interesting issues in high bar gymnastics. Arampatzis and Brüggemann [1] analysed the energy exchange between bar and gymnast using a three-dimensional 15 segment gymnast body model coupled to a high bar with 12 inter-connected rigid elements. Yeadon and Hiley [2] used a much simpler planar model to investigate the fundamental mechanics of the backward giant circle, with a damped linear spring connected to a four

[1] Experimental data and a preliminary version of the high bar - gymnast model presented herein were part of the author's unpublished Dr. Scient. Thesis "Modelling and Analysing the high bar – gymnast system", The Norwegian School of Sport Sciences, 2001.

segment gymnast body model. They later used this model to examine the margin for error in timing the release for high bar dismounts [3], and a similar model [4] to elaborate on triple somersault dismounts [5], [6]. Some aspects of their model were recently improved somewhat by Begon et al. [7], who presented a 3D model with an extra rotational joint between the torso and the pelvis to study the estimation of high bar kinematics when the number of skin markers is limited. Their model also included a personalised behaviour of the scapular girdle elevation as a function of arm flexion. Sheets and Hubbard [8] also used a four segment (female) gymnast model attached to a damped linear spring when they modeled swinging on the uneven parallel bars.

In these previous works, the high bar part of the model was designed to capture bar bending. However, as was shown by Linge and Hallingstad [9], horizontal movement of bar *endpoints* add substantially to the dynamics of the system. In fact, the absolute horizontal movement of the bar midpoint is composed of bar bending *and* another 30% due to endpoint movement. Also, previous works have been less concerned about robustness of model performance to errors in parameter values. Yet, measurement and parameter estimation errors represent a common challenge to mathematical modeling, being problematic if a model is too sensitive in this respect.

In this paper, a gymnast - high bar model that includes the horizontal dynamics of bar endpoints is presented. The planar three-spring high bar model of Linge and Hallingstad [9] is extended with a 5 segment gymnast body model and the sensitivity of model performance to perturbations in model parameter values is elaborated on.

2 Methods

2.1 Data collection and data processing

A gymnast from the Norwegian Men's Senior Gymnastics Squad gave informed consent to perform giant swings on the high bar while his movements were recorded (frequency $240\,Hz$) with a

ProReflex reflective marker recording system [10]. A total of four giant swings were recorded with 7 cameras that were placed evenly around the bar at a distance of $6\,m$ from the bar midpoint. One giant swing was used for estimation and one for validation. Reflective markers (diameter $12\,mm$) were attached to the bar and to the body, giving symmetry in marker location to each side of the vertical plane through the bar midpoint. Body markers were attached on each side of the body, wrist ($0.05\,m$ proximal to the Processus styloideus ulnae), elbow (Lateral epicondyle), shoulder (Deltoideus posterior), lowest rib (lateral 10^{th} Costa), hip (trocanter major), knee (Lateral epicondyle) and ankle (Lateral malleolus). Reflective markers were placed also on each end of the bar (on top of each vertical post) and on the bar midpoint between the hands of the gymnast. The bar markers allowed the absolute movement of bar endpoints to be measured, as well as the motion of bar midpoint relative to the endpoints.

Collected marker data was filtered with the generalized cross validation algorithm of Woltring [11], choosing a cut-off frequency of $12\,Hz$. Pair wise corresponding positions, velocities and accelerations of markers from the left and right side of the body (and bar) were averaged after projection into the vertical sagittal plane through the midpoint marker on the bar. Kinematics of body joints was derived from the averaged data in the symmetry plane. Data processing and parameter estimation were done in Matlab [12].

2.2 High bar - gymnast model

The 2D high bar model of Linge and Hallingstad [9] was extended with a planar 5 segment gymnast body model, generating the dynamic equations for the total model (Figure 1) with ROBMAT [13]. In the high bar model of Linge and Hallingstad [9], the horizontal motion of bar endpoints is included so that three damped linear springs are used to model bar dynamics, two springs horizontally and one vertically. In this way, bar midpoint motion can be represented relative to the moving endpoints of the

bar. Each of the three high bar springs has a stiffness, damping and mass parameter, giving 9 parameters in total for the high bar part of the model.

Regarding the gymnast part of the model, each body segment (arms, torso, lower back, thighs and shanks) was assumed to be rigid and defined by its mass, length, inertia and center of mass location on the segment axis. The length of the arms was designed as a joint variable (as part of modeling the shoulder joint, see below); however, so 19 parameters define the five body segments. Segment mass (marker) positions were projected into the sagittal plane, and each segment had markers at each end. Body kinematics could then be derived from segment markers. Angles between segments were used as body joint variables. The shoulder joint, however, is more complicated, and was modeled by two degrees of freedom, both being actively controlled by the gymnast. This might be motivated as follows. An individual holding his arms straight out in front of him is able to change the effective length of the arms purely by shoulder activity while maintaining a fixed shoulder angle. It may be done at any shoulder angle and justifies modeling shoulder configuration with two degrees of freedom, one translatory (q_5 in Figure 1) and one rotational (q_6 in Figure 1). This differs from Yeadon and Hiley (2000) and Sheets and Hubbard (2008), who modeled translatory shoulder action (corresponding to q_5 here) with a passive spring – damper. The distance between the bar midpoint marker and the shoulder marker corresponded to this translatory shoulder motion component. To avoid complicating the model, the variable length of the arms was combined with fixed parameter values for the mass, center of mass position and inertia of the arms. This approximation was based on the assumption that the $5-10\,cm$ length change of the arms would not affect these parameters significantly. Body joint kinematics was used as input to the model while the position of the gymnast was given by the angle of his arms relative to the vertical. Zero friction was assumed between the bar and the hands of the gymnast.

2.3 Parameter estimation and model validation

Body segment parameter values were estimated by the method of Yeadon [14], using the body density values of Dempster [15]. The high bar used in the present study, was the same as the one of Linge and Hallingstad [9]. However, even if they identified optimal bar parameters, they did so by use of a freely oscillating bar, i.e. without an interacting gymnast. Since other bar dynamics effects might come into play with a performing gymnast, bar parameters were estimated anew with the Nelder-Mead simplex method [16] in Matlab. Keeping body segment parameter values fixed, high bar parameter values were estimated by fitting (minimizing rms errors) bar positions and arms angle of the model to corresponding measurements while the gymnast swung through the lower half (horizontal to horizontal) of a regular giant swing. rms errors from bar endpoint and midpoint positions, and arm's angle position, were made to give approximately equal contributions during estimation. To avoid local minima, the estimation was initiated from different places in the parameter search space, distributing starting values around the reference values naturally chosen as the original bar parameter estimates (Table 1) of Linge and Hallingstad [9]. After having estimated bar parameters, validation was carried out with another recording of a giant swing, but now using (more than) a complete giant swing. This swing was defined to start $40°$ before the vertical, go full circle, and end $20°$ after the vertical. Simulated and measured angular positions of the centre of mass (relative to neutral bar position) were compared, and the rms error of bar position was found. Raw measurement data were used for comparison both during estimation and validation.

2.4 Sensitivity analysis

The sensitivity of bar endpoint and midpoint positions, and arms' angle with the vertical, was investigated for the lower half (horizontal to horizontal) of a regular giant swing by perturbing single parameter values and combinations of parameter values. For each of the parameter perturbation trials,

the rms errors of bar positions and arms' angle were calculated, using a simulation for the lower half of the giant swing as a reference. Use of rms errors was preferred over sensitivity functions since it is a compact measure, and the investigations of sensitivity to combinations of parameter perturbations became much simpler.

Matlab scripts were designed for three sets of sensitivity studies. First, the rms error sensitivity to single parameter perturbations ($+10\%$) was investigated for each of the 28 high bar and body segment parameters given in Table 2. The order of perturbations followed the lines of this table, i.e. with k_1 being the first parameter modified, k_2 the second, and so on, until I_5 was changed as the last one. In the second set of sensitivity tests, all combinations of the 9 high bar parameters were tested, keeping body parameters fixed. Each parameter value was allowed to take on three values, either no change from the optimal value, or a $\pm 10\%$ change. This gave $3^9 = 19\,683$ combinations in all, corresponding to equally many simulation trials, with the order of perturbations chosen as follows. All high bar parameters were started at optimal values, and perturbations started with the last parameter (Table 2), i.e. m_3. This was followed by all combinations of m_2 and m_3, and so on. This scheme implied for example that $3^8 = 6561$ simulation trials were run for each value of k_1, $3^7 = 2187$ trials were run for each value of k_2 and that $3^6 = 729$ trials were run for each value of k_3. Finally, in the third set of sensitivity tests, combinations of both high bar and body parameter values were analysed. Since the total problem would have been too large (3^{28} parameter value combinations), it was reduced by selecting a subset of combinations only. In the first set of sensitivity studies, it was seen that of the high bar parameters; bar position sensitivity was noticeably higher for the three stiffness values than for damping and mass parameters. The three bar stiffness parameters were therefore used in combination with segment parameters from the arm, torso and thigh segments, taking these segments to be representative for the influence of perturbed body segment parameters. In addition, each parameter was allowed to take on just two values, either no change or a $+10\%$ change. The number of combinations was such reduced to $2^{14} = 16384$. With reference to Table 2, the parameters involved in this set of sensitivity testes were then $k_i, i = 1,2,3$, from the bar parameters, and all body

segment parameters (capital letters) except those with indices 3 and 5, which corresponds to not perturbing the lower back and shaft segment parameters. Again, for the order given, perturbations were started at the end of the (subset) list, i.e. first with I_4 only, then I_2 and I_4, and so on, changing k_1 as the last one. This means that, e.g., $2^{13} = 8192$ simulation trials were run for each value of k_1, $2^{12} = 4096$ trials for each value of k_2 and $2^{11} = 2048$ trials for each value of k_3. By plotting rms errors as a function of trial number, the known permutation order allowed jumps in rms errors to be coupled with changes in certain parameters.

3 Results

Parameter estimation caused some tuning of high bar parameters, but only for the stiffness and damping parameters of the horizontal direction (Table 1). Damping parameters changed the most, with endpoint damping (c_1) and midpoint damping (c_2) being reduced by 50% and 30%, respectively. Horizontal endpoint stiffness (k_1) was reduced by 2% and midpoint stiffness (k_2) by 13%. rms errors during estimation were $0.004m$, $0.013m$, $0.013m$ and $5.7°$, for horizontal bar endpoint position, horizontal bar midpoint position (relative endpoints), vertical bar midpoint position and, finally, arms' angle with the vertical, respectively. Note that the high bar used for the present studies was only used for training sessions, and vertical stiffness values (Table 1) were above the range ($19620 - 23980\,Nm^{-1}$) used in competitions. Note also the somewhat counter-intuitive stiffness values of Table 1, particularly for the freely oscillating bar, having substantially higher stiffness horizontally as compared to vertically. One would reasonably expect the stiffness values to be more equal since the bar itself is homogeneous with the same circular cross-section all along its length. However, the bar itself does not stretch, and can only bend because endpoints move towards each other. Furthermore, because of the apparatus design, bar endpoints move differently when the bar

bends horizontally as compared to vertically (Linge and Hallingstad [9]). As a result, stiffness values may differ considerably with direction.

Model validation (Figure 2) demonstrated that the simulated angular position of the centre of mass with respect to neutral bar position remained close (rms difference $< 11°$) to measurements for almost the entire inverval. After about $1.5\,s$, model prediction deteriorated as the model began to rotate too fast. The rms errors for the horizontal ($q_1 + q_2$) and vertical (q_3) bar positions were $0.017\,m$ and $0.015\,m$, respectively. It was confirmed (not shown) that the vertical deviation of bar endpoints was negligibly small ($< 1\,mm$). The good match between simulation and measurement demonstrated that simulated angular momentum and centre of mass velocity were in close agreement with measurements.

The reference simulation (Figure 3) of the sensitivity analysis showed in more detail how well bar kinematics and arm angle were predicted by the model over the reference interval when estimated parameters were used. Rms errors were $0.004\,m$, $0.011\,m$, $0.011\,m$ and $4.6°$, for q_1, q_2, q_3 and q_4 (Figure 3a – d), respectively. The horizontal contribution (Figure 3a) of bar endpoints added almost 30% to the horizontal position component caused by bar bending (Figure 3b). It was noted that as the gymnast passed the lowest position under the bar, model prediction of bar midpoint positions (Figures 3b and 3c) had the largest errors.

Single parameter perturbations (Figure 4) illustrated that bar position variables were most negatively influenced (rms errors $< 0.006\,m$) by modifications in spring constants (k_1, k_2, k_3), and that segment length (L_2, L_3, L_4, L_5) adjustments had the greatest impact on the arms' angle (rms error $< 0.9°$). When combining high bar parameter perturbations (Figure 5), the rms error for q_1 (Figure 5a) was still found to be small ($< 0.002\,m$) for all trials, but slightly elevated when k_1 was modifed by $\pm 10\%$, i.e. during the last ($2 \times 3^8 =$) 2×6561 trials. The rms errors for q_2 ($< 0.007\,m$), q_3 ($< 0.008\,m$) and q_4 ($< 1.2°$) were also small, with patterns that were more or less repeated for each value of k_1, but with distinct changes as k_2 and k_3 were modified, i.e. with every ($3^7 =$) 2187 and

($3^6 =$) 729 trials, respectively. rms errors for q_4 were larger for combinations of high bar parameter value perturbations (Figure 5d) than for isolated perturbations of segment lengths (Figure 4d). For combinations of high bar and body segment parameter perturbations (Figure 6), rms errors for bar positions ($< 0.006\,m$) and arms' angle ($< 1.8°$) were still small. Again, patterns in rms errors matched shifts in k_1, k_2 and k_3, which took place for every ($2^{13} =$) 8192, ($2^{12} =$) 4096 and ($2^{11} =$) 2048 trial, respectively.

4 Discussion

In this paper, a new 2D gymnast - high bar model that includes horizontal bar endpoint dynamics was presented. A three-spring high bar model [9] was extended with a 5 segment gymnast model followed by validation and sensitivity analysis. The total model was able to predict high bar kinematics and gymnast angular position with good accuracy. It was found that for minor errors (10%) in parameter values, model performance was most sensitive to high bar stiffness values, but the model still performed well, even for combinations of parameter errors.

Our model is planar like the one of Hiley and Yeadon [4], but has an extra rotational joint between the torso and pelvis, as Begon et al. [7] included in their 3D high bar - gymnast model. The present model differs from the models of Hiley and Yeadon [4] and Begon et al. [7] in the way the high bar and the shoulder joint are represented. The shoulder joint is complicated, and Hiley and Yeadon [4] showed that its translatory component might be captured well by use of a damped linear spring. Begon et al. [7] handled it somewhat differently, by letting the scapular girdle elevation be a personalised function of arm flexion. Here, it has been shown that the translatory and rotational properties of the shoulder also might be treated as two independent joint variables. The accuracy of the present model was comparable to that achieved by Yeadon and Hiley (2000) for the angular position

of the centre of mass. They evaluated their model for a giant swing covering an inverval of $450°$, i.e. about the same as the $440°$ used here (Figure 2). In their case, they got an rms difference between simulated and measured time histories of $9°$, compared to $11°$ with the present alternative (2.5% of the total rotation angle). As in the present work, their model predicted the angular position very well for the first $1.5s$, after which the simulated rotation became too fast. When predicting horizontal and vertical bar positions over the interval, Yeadon and Hiley (2000) achieved rms errors of $0.009m$ and $0.007m$, respectively, which is better than the corresponding figures $0.017m$ and $0.015m$ of the present study. Sheets and Hubbard (2008), who developed a model similar to the one of Yeadon and Hiley (2000) for female swings on the uneven parallel bars, also achieved a better rms error ($0.006m$), though for a smaller angular interval of $270°$. Even if the bar position rms errors are larger in the present work, they are still small, considering the high bar diameter of $0.03m$. Why the present model produced higher bar position rms errors than previous models is not clear. Some of the explanation might be found in different equipment and procedures of the studies. The kind of exercise being modelled is another thing, since different exercises might favorise different aspects of a model. More degrees of freedom might be required to model more violent moves like, e.g., release-regrasp exercises. None of the previously presented models have been subject to sensitivity analysis, so how well they perform with non-optimal parameters is not yet clear.

High bar endpoints added another 30% to the horizontal displacement component of the bar midpoint obtained from bar bending alone, just as Linge and Hallingstad [9] reported for free high bar oscillations. Linge and Hallingstad [9] validated the high bar model for free oscillations in the horizontal and vertical directions separately. Here, it has been shown that the high bar part of the model also performs well with a swinging load, i.e. when a performing gymnast imposes *simultaneous* horizontal and vertical high bar motion. However, some tuning of high bar parameters was necessary, suggesting that high bar dynamics differ somewhat when a gymnast is performing in it, compared to the situation when oscillations are free. It was noted that high bar kinematics predicted by the model differed the most from measurements (Figure 3) as the gymnast passed through the lowest part of the

giant swing. This is at the time when bar bending and endpoint movement is at its largest, suggesting that some unmodeled effects remain in the 3D system.

The rms error was used as a sensitivity measure even though such a number does not convey as much detail as the whole time series of a sensitivity function. However, some compact measure like the average or maximum absolute value would still have to be extracted from each sensitivity function time series to compare the impacts of different parameter perturbations. The rms error is a compact measure and convenient to use when combinations of parameter errors are investigated.

Sensitivities to combinations of parameter value perturbations should preferably have been studied by considering *all* parameter value combinations, rather than just subsets of combinations as done in this work. However, changing each of the 28 parameters by 0, -10% or $+10\%$ gives 3^{28} possibilities, and even a one-sided perturbation by $+10\%$ gives 2^{28} possibilities, which is still very big for practical analysis. In the final set of sensitivity tests, damping and mass parameters of the high bar were left out, and also parameters for the lower back and shaft segments. This gave rms errors $< 0.008\,m$ for bar positions and an rms error $< 1.8°$ for the arms' angle, which is acceptable for most purposes. The rms errors for the complete problem, i.e. with all 28 parameters, are likely to be somewhat higher. However, they are still expected to be acceptable, since, e.g., a doubling of rms errors would still be tolerable for most model applications. In our results, the influence of leaving out bar damping and mass parameters can be seen by comparing rms errors for vertical bar position in the two final sensitivity tests (Figures 5c and 6c). Assuming for a moment that *all* high bar parameters had been kept while including body segment parameter perturbations, the rms errors in the final sensitivity test (Figure 6c) should have been at least as high as before (Figure 5c). In our case, however, they are slightly reduced. The choice of $\pm 10\%$ perturbations was made, but it is realized that other choices (e.g. 5% or 15%) might have influenced the results, first and foremost the relative importance of parameters, not the overall robustness of the model.

Sheets and Hubbard (2008) reported that active shoulder modeling and an extra torso joint could have improved their model. The present model includes both these aspects, as well as a more

detailed model of the apparatus dynamics. Furthermore, as has yet to be shown for the previously presented models, it is robust to changes in parameter values.

5 Conclusion

A new 2D gymnast - high bar model was developed. As opposed to previous models, this model includes the substantial horizontal movement of bar endpoints that adds to motion from pure bar bending. Model performance was found most sensitive to errors in high bar stiffness values, but is still robust to minor errors (10%) in its parameter values.

Conflict of interest statement

The authors declare that they have no conflict of interest.

Acknowledgements

Thanks to the Norwegian School of Sport Sciences for financing early stages of this work. Many thanks to Flemming Solberg for contributing with his European top level gymnastic skills. Also thanks to Olaf Steinsland, Flemming Solberg, Tron Krosshaug, Michael Guttormsen and Oddvar Hallingstad for helpful discussions.

References

1. Arampatzis A, Brüggemann GP (1998) A mathematical high bar - human body model for analysing and interpreting mechanical - energetic processes on the high bar. Journal of Biomechanics 31: 1083-1092
2. Yeadon MR, Hiley JH (2000) The mechanics of the backward giant circle on the high bar. Human Movement Science 19: 153-1
3. Hiley JH, Yeadon MR (2003a) The margin for error when releasing the high bar for dismounts. Journal of Biomechanics 36: 313-319

4. Hiley JH, Yeadon MR (2003b) Optimum technique for generating angular momentum in accelerated backward giant circles prior to a dismount. Journal of Applied Biomechanics 19: 119-130
5. Hiley JH, Yeadon MR (2005) Maximal dismounts from high bar. Journal of Biomechanics 38: 2221-2227
6. Hiley JH, Yeadon MR (2008) Optimization of high bar circling technique for consistent performance of a triple piked somersault dismount. Journal of Biomechanics 41: 1730-1735
7. Begon M, Wieber PB, Yeadon MR (2008) Kinematics estimation of straddled movements on high bar from a limited number of skin markers using a chain model. Journal of Biomechanics 41: 581-586
8. Sheets AL, Hubbard M (2008) Evaluation of a subject-specific female gymnast model and simulation of an uneven parallel bar swing. Journal of Biomechanics 41: 3139-3144
9. Linge S, Hallingstad O (2002) Gymnastics - a new 2D model of the high bar including endpoint movement, Sports Engineering 5: 81-92
10. Qualisys Medical AB, Adaptive Optics Associates, Inc. (1999) QTracCapture for Microsoft Windows (Version 2.5)
11. Woltring HJ (1986) A Fortran package for generalized, cross-validatory spline smoothing and differentiation, Adv. Eng. Software 8: 104-113
12. The MathWorks Inc. (1999) Matlab for Microsoft Windows (Version 5.3.0.10183 (R11)).
13. Horn G, Linge S (1994) Analytical generation of the dynamical equations for mechanical maipulators, The Mathematica Journal 4**:** 67-73
14. Yeadon MR (1990) The simulation of aerial movement, Part II: A mathematical inertia model of the human body. Journal of Biomechanics 23: 67-74
15. Dempster WT (1955) Space requirements of the seated operator. WADC-55-159, AD-087-892. Wright-Patterson Air Force Base, Ohio, U.S.A.
16. Nelder JA, Mead R (1965) A simplex method for function minimization. Computer Journal 7: 308

Table 1 High bar parameter values estimated in the high bar - gymnast model. Reference values are the ones estimated for a freely oscillating bar (Linge and Hallingstad, 2002).

	k_1 (N/m)	**c_1 (Ns/m)**	**m_1 (kg)**	**k_2 (N/m)**	**c_2 (Ns/m)**	**m_2 (kg)**	**k_3 (N/m)**	**c_3 (Ns/m)**	**m_3 (kg)**
Reference	122606.0	207.0	15.2	32452.0	21.0	2.1	27665.0	14.0	5.7
Estimate	120000.0	100.0	15.2	28200.0	15.0	2.1	27665.0	14.0	5.7

Table 2 Parameter matrix where k_i, c_i m_i, $i = 1,2,3$, denote the nine high bar parameters (see Figure 1). Capital letters are used for body segment parameters, with M_i, L_j, R_i, I_i, $i = 1,...,5$, $j = 2,...,5$, denoting mass, length, center of mass position along segment axis and inertia, respectively. The arms, torso, lower back, thighs and shafts body segments are numbered consecutively from 1 to 5, corresponding to the sub indices of body parameters. There is no L_1 parameter since the length of the arms is a model variable.

k_1	k_2	k_3	c_1	c_2	c_3	m_1
m_2	m_3	M_1	M_2	M_3	M_4	M_5
L_2	L_3	L_4	L_5	R_1	R_2	R_3
R_4	R_5	I_1	I_2	I_3	I_4	I_5

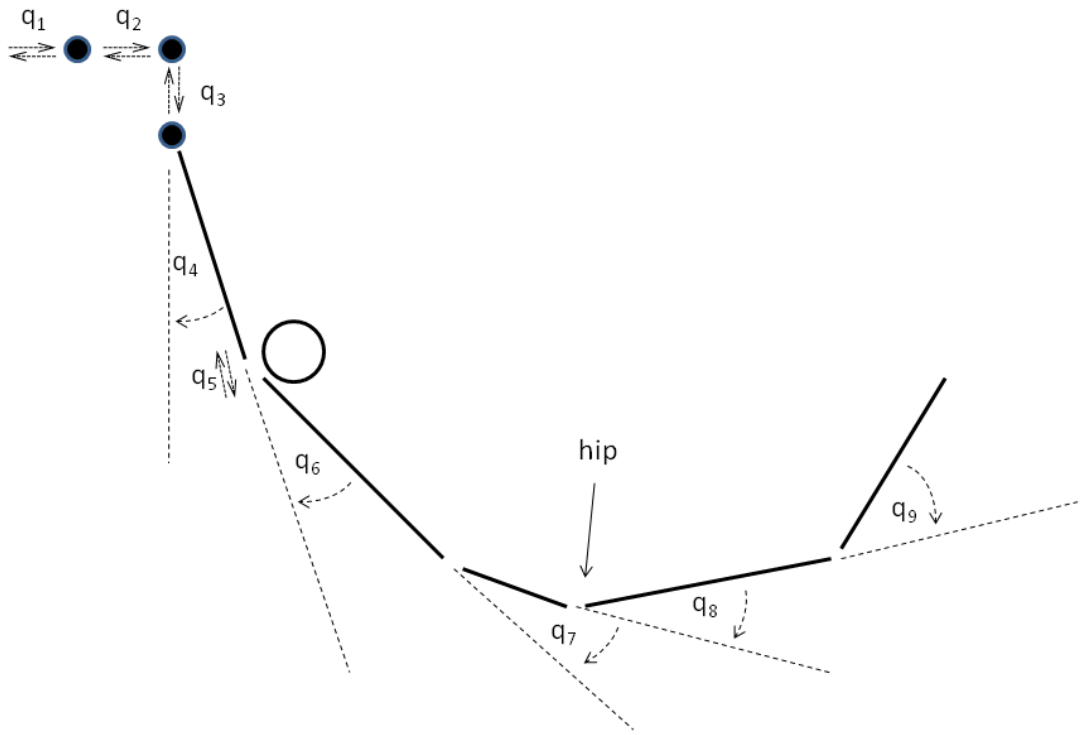

Figure 1 The planar high bar - gymnast model with 9 degrees of freedom $q_i, i = 1,2,...,9$. Variable q_1 represents the absolute horizontal position of bar endpoints, q_2 is the horizontal position of bar midpoint relative endpoints, q_3 denotes the vertical position of bar midpoint, q_4 is the angle of the arms with the vertical, q_5 is the length of the arms (which changes because of translatory shoulder motion), q_6 is the angle between arms and trunk segment, q_7 is the angle between trunk and lower back segments, q_8 is the hip angle, and, finally, q_9 is the knee angle. Variables q_1, q_2 and q_3 represent the positions of the three damped linear springs that make up the high bar part of the model, having mass-components indicated with filled circles here.

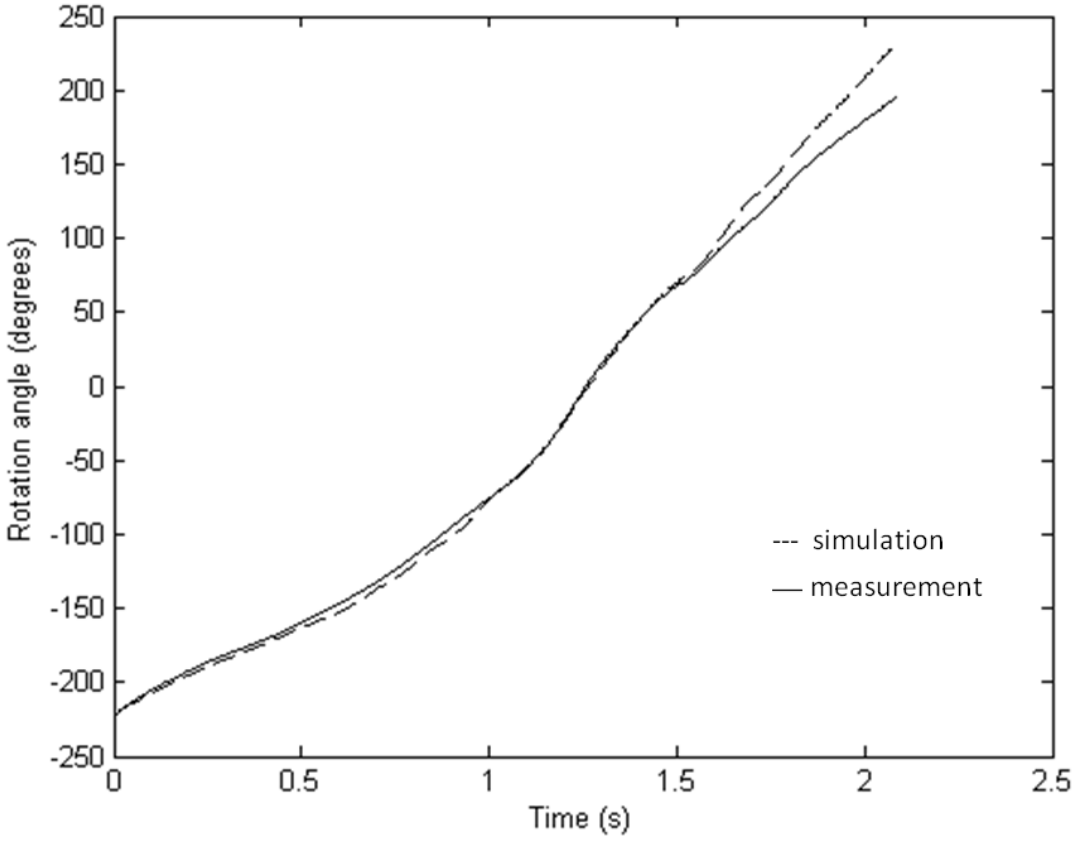

Figure 2 Angular position of the centre of mass during (more than) a complete giant swing started $40°$ before the vertical (handstand) and ended $20°$ after.

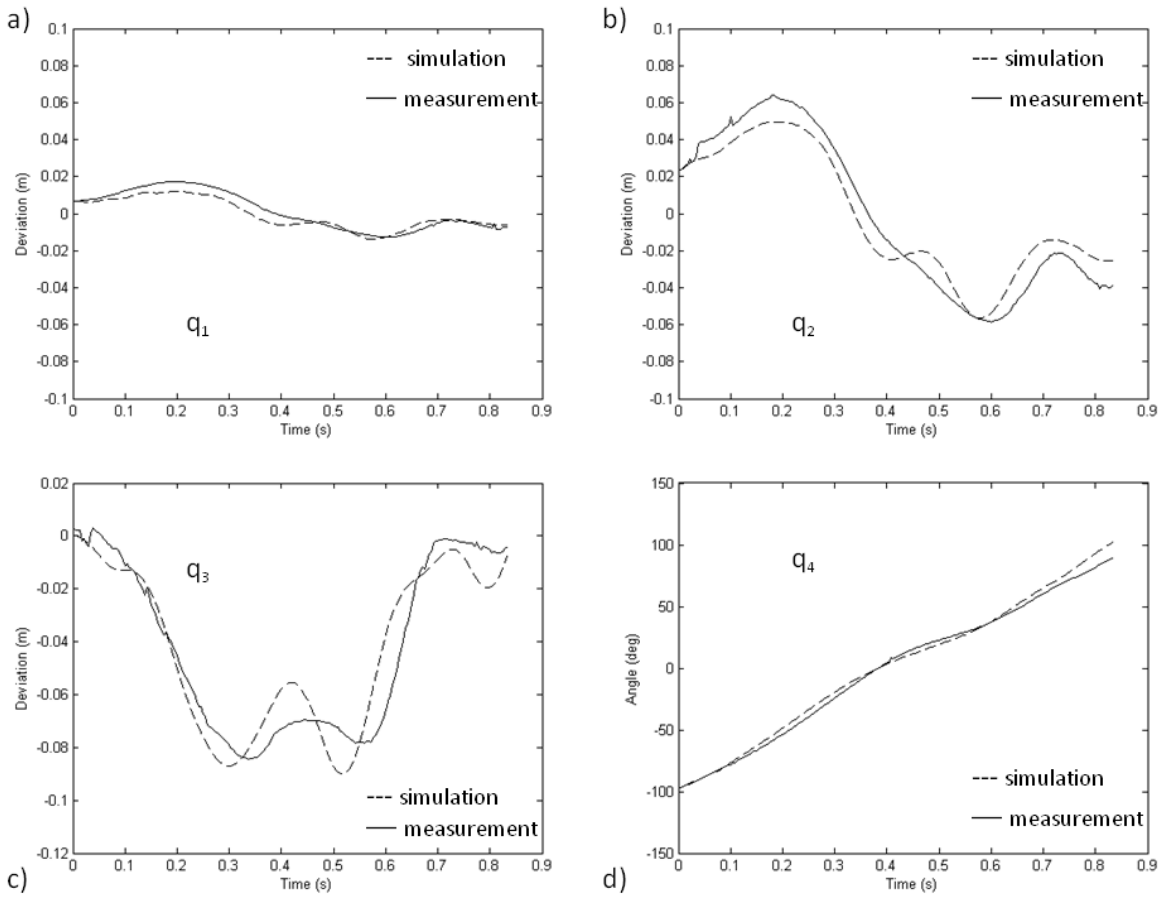

Figure 3 Bar position and arm angle for the lower half (horizontal to horizontal) of a simulated giant swing used as reference for the sensitivity analysis, a) variable q_1 represents horizontal position of bar endpoints, b) q_2 is horizontal position of bar midpoint relative endpoints, c) q_3 denotes vertical position of bar midpoint and d) q_4 is the angle of the arms with the vertical. Corresponding measurements are shown for comparison.

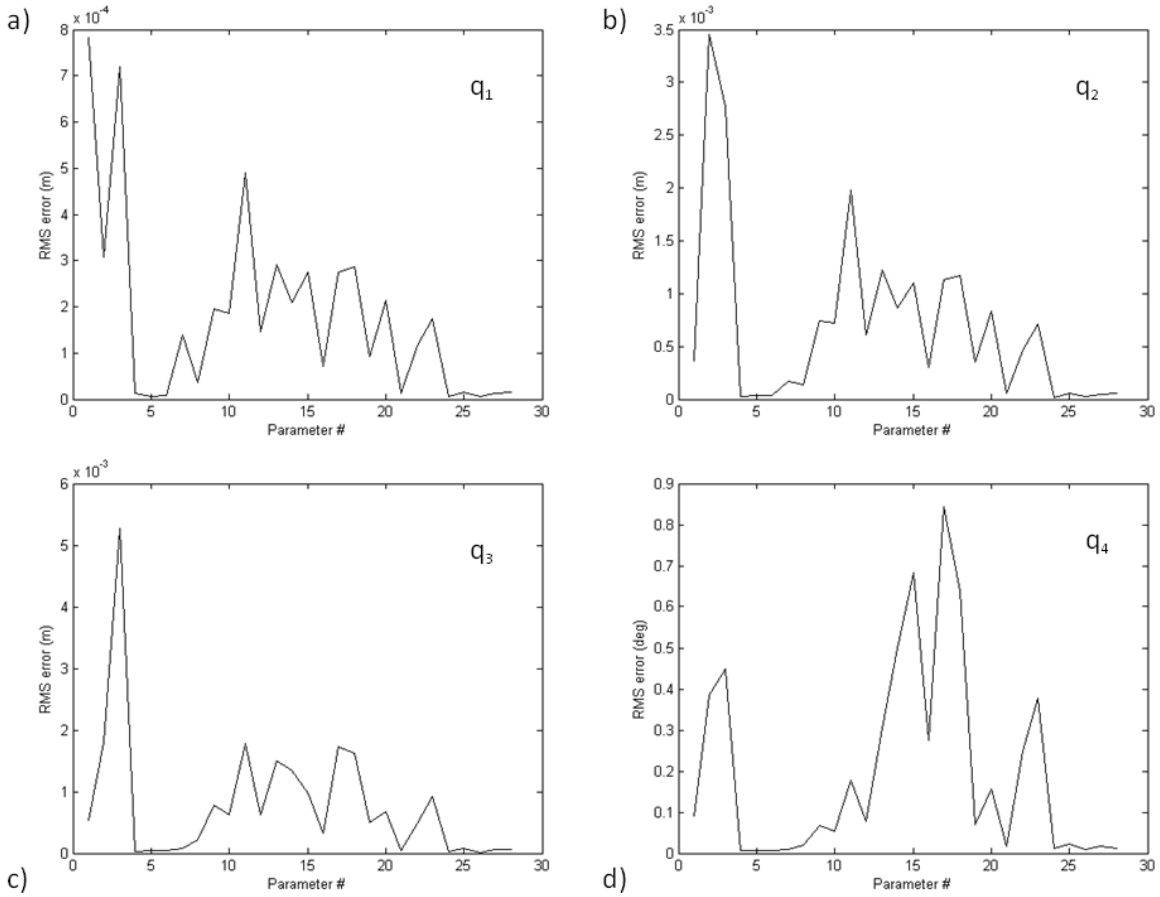

Figure 4 RMS error, a) - d), as a function of parameter number using the validation simulation run as a reference. All 28 bar and body parameters values (Table 2) were numbered consequtively from the bar towards the feet and only one pararameter values was changed ($+10\%$) at a time. Variable q_1 represents horizontal position of bar endpoints, q_2 is horizontal position of bar midpoint relative endpoints, q_3 denotes vertical position of bar midpoint and q_4 is the angle of the arms with the vertical. Note the difference in scaling for the vertical axis of a) compared to b) and c).

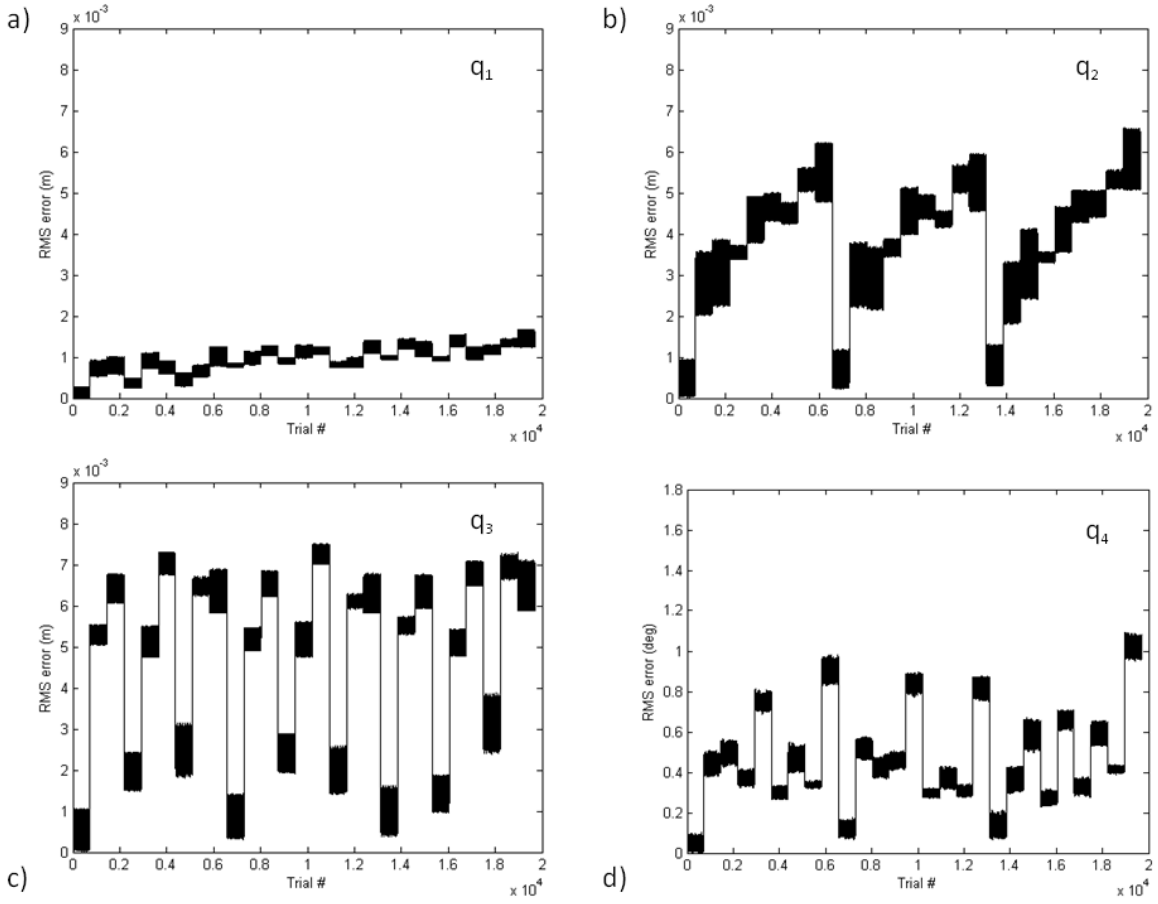

Figure 5 RMS error, a) - d), as a function of trial number where one trial represents one particular combination of high bar parameter values. Body parameter values were kept fixed. The validation simulation run was used as a reference. Each of the 9 high bar spring parameters could take on three values, the estimated value and $\pm 10\%$, giving a total of $3^9 = 19683$ combinations, i.e. trials. Variable q_1 represents horizontal position of bar endpoints, q_2 is horizontal position of bar midpoint relative endpoints, q_3 denotes vertical position of bar midpoint and q_4 is the angle of the arms with the vertical.

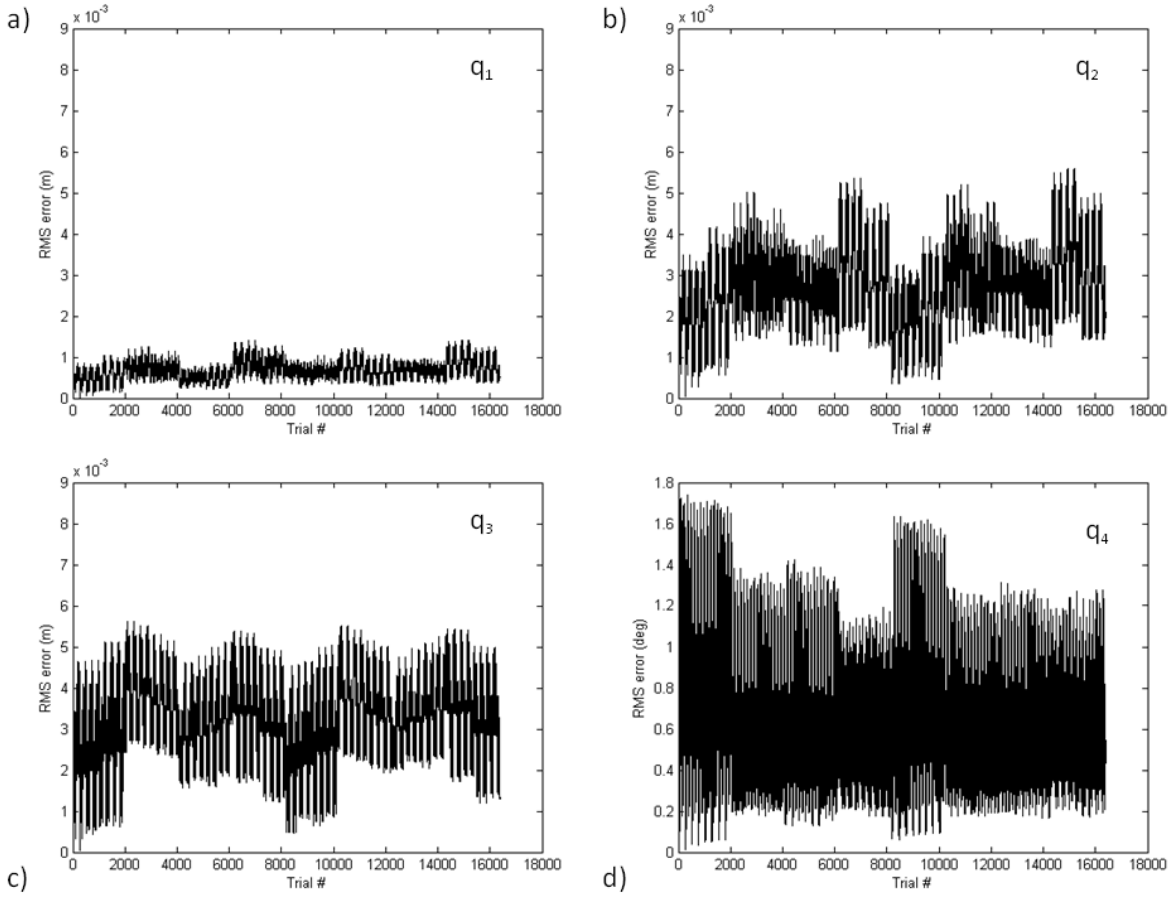

Figure 6 RMS error, a) - d), as a function of trial number where one trial represents one particular combination of high bar and gymnast body parameter values. The validation simulation run was used as a reference. Selected bar and body segment (arms, torso and thighs) parameters were allowed to take on two values, the estimated one and + 10%, giving $2^{14} = 16384$ combinations in all. Variable q_1 represents horizontal position of bar endpoints, q_2 is horizontal position of bar midpoint relative endpoints, q_3 denotes vertical position of bar midpoint and q_4 is the angle of the arms with the vertical.